How to cite: *Angew. Chem. Int. Ed.* **2022,** *61,* e202207532
International Edition: doi.org/10.1002/anie.202207532
German Edition: doi.org/10.1002/ange.202207532

Solid-Phase Synthesis

Versatile Synthesis of Multivalent Porphyrin–Peptide Conjugates by Direct Porphyrin Construction on Resin

Yue Wu, Ho-Fai Chau, Yik-Hoi Yeung, Waygen Thor, Hei-Yui Kai, Wai-Lun Chan, and Ka-Leung Wong**

Abstract: Multifunctional porphyrin–peptide conjugates with different propensities for self-assembly into various supramolecular nanoarchitectures play important roles in advanced materials and biomedical research. However, preparing prefunctionalized core porphyrins by traditional low-yielding statistical synthesis and purifying them after peptide ligation through many rounds of HPLC purification is tedious and unsustainable. Herein, we report a novel integrated solid-phase synthetic protocol for the construction of porphyrin moieties from simple aldehydes and dipyrromethanes on resin-bound peptides directly to form mono-, *cis*/*trans*-di-, and trivalent porphyrin–peptide conjugates in a highly efficient and controllable manner; moreover, only single final-stage HPLC purification of the products is needed. This efficient strategy enables the rapid, greener, and substrate-controlled diversity-oriented synthesis of multivalent porphyrin–(long) peptide conjugate libraries for multifarious biological and materials applications.

Introduction

Porphyrin derivatives, a typical class of tetrapyrrole macrocycles, illustrating myriad fascinating photophysical, chemical and biological properties, e.g., fluorescence, metal ions chelation, aggregation, and reactive oxygen species generation, lend themselves as a versatile molecular platform in a wide range of light-harvesting, photocatalytic, biomedical, supramolecular, and framework/nano-materials research. Upon combining with peptides, the water solubility, the biocompatibility, the biostability, the biotarget specificity, as well as the self-assembly properties of the global porphyrin–peptide systems[1] would change, allowing such conjugates to be wisely and widely employed as fluorescent bio-probes,[2,3] targeted photodynamic therapy (PDT) agents,[4–6] artificial metalloenzymes,[7,8] as well as the building blocks for biofunctional self-assembling nanostructures.[9–14] In addition, the D_{4h} symmetry point group of porphyrins with four *meso*-positions allows their peptide conjugates to be ideal templates for the multivalent approach[15] (i.e., multiple bioactive peptide chains can be attached to a core porphyrin scaffold). This approach has been well-substantiated as a feasible strategy to improve the binding affinity and selectivity of diagnostic/therapeutic agents for various ligand–receptor interactions (e.g., cyclic RGD peptides to integrins) as they showed significantly improved performance compared with the corresponding monovalent counterparts.[16–22]

The conventional synthetic approaches to porphyrin–peptide conjugates have been well-summarized and reviewed,[23] which can be simply classified into solid-phase conjugation (incorporating a –COOH containing porphyrin building block onto *N*-terminal or unprotected lysine side chain in most cases) and site-specific solution-phase ligation (e.g., copper(I)-catalyzed alkyne-azide cycloaddition CuAAC, maleimide-thiol reactions) (Figure 1a). However, all the methods to synthesize porphyrin-peptide conjugates cannot be performed without using pre-functionalized porphyrin building blocks, which possess one or more functional groups for conjugation. In fact, such building blocks are expensive in limited commercial sources as needed are very tedious statistical synthetic procedures of "pyrrole chemistry" that usually suffer from lots of side reactions and difficulties in purification—due to the serious aggregation issue. For modern advanced biological and materials research that would involve porphyrin–peptide conjugates with different valency (both monovalent and multivalent) for comparing the multivalent effect of peptides on their targets and developing supramolecular aggregated or framework systems, more challenging and low-yield symmetrical/non-symmetrical pre-di/tri/tetra-functional porphyrin starting materials have to be secured beforehand, which can be nightmares from the synthetic chemistry perspective. On the other hand, solid-phase peptide synthesis (SPPS) is the most practical and well-established approach for preparing peptides and their derivatives in both laboratories and industries.[24–26] In Fmoc-SPPS (with

[*] Dr. Y. Wu, Dr. H.-F. Chau, Y.-H. Yeung, W. Thor, H.-Y. Kai, Prof. Dr. K.-L. Wong
Department of Chemistry, Hong Kong Baptist University
224 Waterloo Rd, Kowloon Tong, Kowloon, Hong Kong SAR (China)
E-mail: klwong@hkbu.edu.hk
Prof. Dr. W.-L. Chan
Department of Applied Biology and Chemical Technology, The Hong Kong Polytechnic University
Hung Hom, Hong Kong SAR (China)
E-mail: wai-lun-kulice.chan@polyu.edu.hk

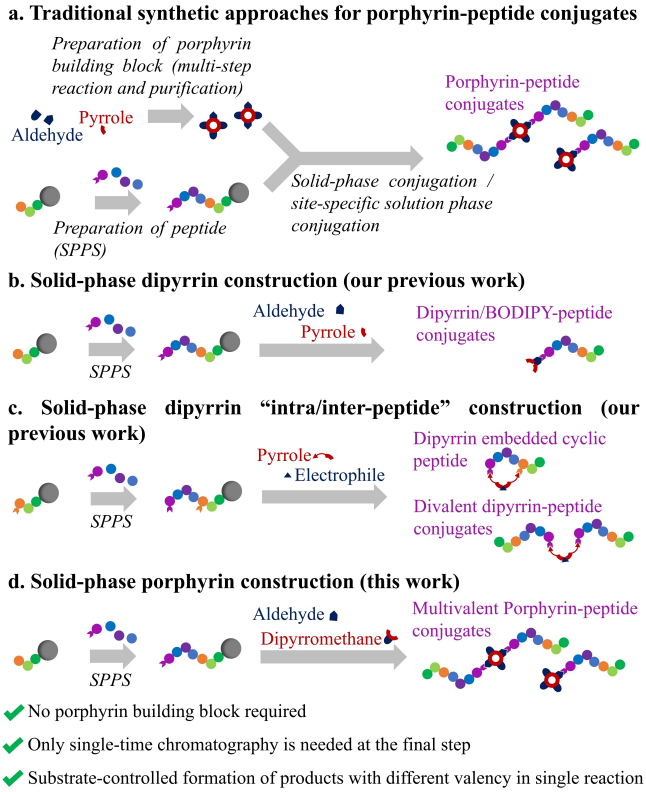

Figure 1. a) Previous synthetic approaches to access porphyrin–peptide conjugates. Functionalized porphyrin building blocks can be conjugated with peptide chains by either solid-phase incorporation or site-specific solution-phase conjugate. b) Our previous work: solid-phase construction of dipyrrin-peptide conjugates.[27] c) Our previous work: solid-phase construction of dipyrrin-embedded cyclic peptide and divalent dipyrrin–peptide conjugates.[28] d) This work: solid-phase porphyrin construction with multivalency.

the fluorenylmethoxycarbonyl protected N-terminus), excess Fmoc-protected amino acids are used for assembling peptide chains, and the Fmoc protecting groups on the latest attached amino acid can be removed to release a free amine for coupling another Fmoc-protected amino acid. As the unbound side-products, as well as those excess reagents/reactants employed to ensure complete conversion for every single step, can be removed by simple washing—i.e., no further purification is required before cleaving peptides from their solid supports.

We therefore hypothesized and proposed that SPPS can be an ideal synthetic platform to be translated for circumventing the long-standing synthetic difficulties of "pyrrole chemistry" which also suffers from excess unreacted reactants, additional reagents, and numerous side-products as above-mentioned. In our recent study in 2020, by condensing the pyrrole building blocks in the solution phase with the newly attached aldehyde linkers on-resin, the dipyrrin-peptide conjugates, which could be applied as target-specific fluorescent probes after boron complexation, were obtained with adequate yields after on-resin oxidation, global cleavage and deprotection (Figure 1b).[27] Moreover, in 2021, we further developed a synthetic approach by linking two newly attached pyrroles on resin together with electrophiles from the solution phase to give the multifunctional dipyrrin-embedded cyclic peptides and divalent dipyrrin-peptide conjugates (Figure 1c).[28] These previous studies prove the "pyrrole chemistry" can be excellently compatible with SPPS for both the condensation between pyrroles and electrophiles, as well as additional treatments like the on-resin oxidation. Therefore, to streamline the workflow and workload for synthesizing porphyrin-peptide conjugates for applications in a wide range of scientific fields, we strive for developing a novel and relatively more green and sustainable integrated approach by directly constructing porphyrin motifs during SPPS.

We herein report a novel procedure-economical methodology for efficiently yielding diverse porphyrin-peptide conjugates of multivalency controlled by the dipyrromethane substrates in use (Figure 1d). The *trans*-divalent porphyrin-peptide conjugates can be prepared with good yield by condensing the relatively stable electron-deficient dipyrromethanes with the newly coupled aldehyde motif on resin-bound peptide chains, while multiple (tri/*cis*-di/monovalent) porphyrin-peptide conjugates can also be obtained in a single reaction when the relatively unstable electron-rich dipyrromethanes was incorporated. This synthetic protocol enables the fast production of multivalent/monovalent porphyrin-(long) peptide conjugate for various biomedical application at wills and provide an efficient diversity-oriented synthesis (DOS) approach to establish libraries for investigating the multivalent effect of peptides toward their targets, as well as their potential formulation into various sizes and shapes of nanoparticles for drug delivery. The given protocol was executed in synthesizing a series of bioactive porphyrin-(long) peptide conjugates, and selected bioimaging applications of some of them were also exemplified.

Results and Discussion

Inspired by the efficient inter-peptide construction of divalent dipyrrin-peptide conjugate in our previous studies (Compound 10 in the corresponding literature),[28] as well as the well-established synthetic approach to synthesize *trans*-divalent porphyrin from dipyrromethanes and aldehydes,[29] the feasibility of on-resin inter-peptide porphyrin construction was initially investigated on RGD peptide, as the model, on Rink amide resin (Figure 2a). The 2-(4-formylphenoxy)acetic acid, a common –COOH containing aldehyde linker, was then attached onto the N-terminus of peptide by routine coupling protocol. The di(1*H*-pyrrol-2-yl)methane (**1a**), a commercially available dipyrromethane building block (5 equiv), was then condensed with an aldehyde on resin under the catalysis of trifluoroacetic acid (TFA) in dichloromethane (DCM) (5 equiv v/v < 1 %; no undesired peptide chain removal was observed). The resin turned red after overnight (≈16 h) condensation in dark, which indicated the formation of porphyrinogen-like moieties on resin. The resin was then treated by oxidant 4,5-dichloro-3,6-dioxo-1,4-cyclohexadiene-1,2-dicarbonitrile

a

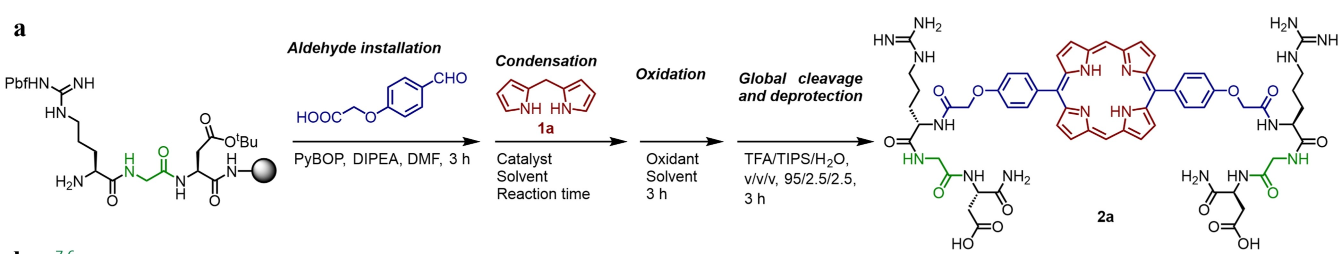

b

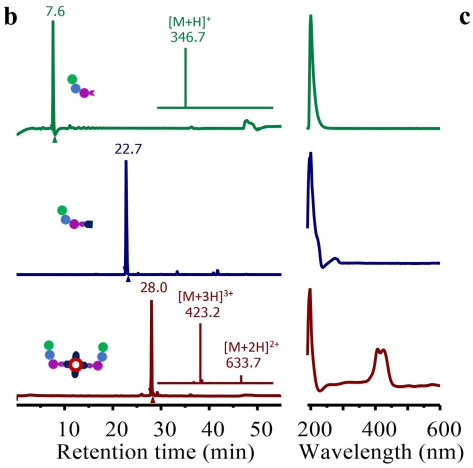

c

Entry	Condensation			Oxidation		HPLC conv. (%) [a]
	Solvent	Catalyst	Reaction time	Solvent	Oxidant	
1	DCM	TFA [b]	16 h	DCM	DDQ	86
2	DMF	TFA	16 h	DCM	DDQ	0
3	DMAc	TFA	16 h	DCM	DDQ	0
4	NMP	TFA	16 h	DCM	DDQ	0
5	DCM	$BF_3{\cdot}OEt_2$ [c]	16 h	NMP	DDQ	83
6	DCM	$BF_3{\cdot}OEt_2$	8 h	NMP	p-chloranil	92
7	DCM	TFA	2 h	NMP	DDQ	28
8	DCM	TFA	8 h	NMP	p-chloranil	92
9	DCM	TFA	40 h	NMP	p-chloranil	91
10	DCM	TFA	16 h	NMP	DDQ	92
11	DCM	TFA	16 h	NMP	p-chloranil	93

Figure 2. a) The reaction scheme of inter-peptide porphyrin construction on resin-bound RGD peptide. b) The step-by-step reaction monitoring for the optimal condition for inter-peptide" porphyrin construction on resin-bound RGD peptide. The reaction was monitored by analytical HPLC (left column) with real-time UV/Vis spectra (right column) and ESI-MS. From top to bottom: untreated RGD peptide cleaved from sampled resin (green), aldehyde-conjugated peptide cleaved from sampled resin (navy) and the crude post-cleavage solution after porphyrin construction (maroon). c) The screening of reaction conditions for inter-peptide porphyrin construction on resin-bound RGD peptide. [a] The conversions were estimated by the HPLC (absorbance at 220 nm) of crude mixture for the percentage of peptide chain(s) involved in the corresponding product. [b] 5 equiv TFA was used (v/v < 1%) in all cases. [c] 1 equiv $BF_3{\cdot}OEt_2$ was used in all cases as undesired peptide chain cleavage was observed under 5 equiv $BF_3{\cdot}OEt_2$.

(DDQ) for 3 h in DCM as our previous studies and cleaved for analysis. As a result, the expected *trans*-divalent porphyrin–peptide conjugate **2a** was obtained as the major product in the crude post-cleavage mixture with around 86 % conversion (Figure 2c, Entry 1). The conversion concept in this work is defined as the percentage of peptide chain(s) involved in the corresponding product by monitoring the absorbance at 220 nm, which is mainly contributed by the peptide bond. The reaction was also analysed by HPLC and ESI-MS step-by-step to demonstrate the perfect conversion of resin-bound peptide under the optimal condition (Figure 2b).

To optimize the reaction, various reaction conditions were investigated. Although resin-bound peptides (especially for the long peptide chains) would swell better in amide solvents [e.g., dimethylformamide (DMF), dimethylacetamide (DMAc) or *N*-methyl-2-pyrrolidone (NMP)], no porphyrin derivative was formed in these solvents (Figure 2c, Entries 2–4). As far as the acid catalyst was concerned, $BF_3{\cdot}OEt_2$ was employed as it was also commonly used for porphyrin synthesis. Undesired peptide chain removal was observed under 5 equiv $BF_3{\cdot}OEt_2$. (v/v ≈ 1.5 %), yet, fortunately, a similar conversion was achieved when 1 equiv $BF_3{\cdot}OEt_2$ was used (Figure 2c, Entry 5 vs. Entry 10; Entry 6 vs. Entry 8). For the reaction time of condensation, after 2 h, only around one fourth peptide chains were consumed, while a comparable conversion of the condensation product could be achieved after 8 h. Longer reaction time (40 h, Figure 2c, Entry 10) showed no obvious improvements as well. We thus preferred to set the condensation reaction for 16 h (overnight) in most of cases for subsequent experiments. For the oxidation step, amide solvent NMP was confirmed to be a better solvent, compared with DCM, as the solubility of oxidants in NMP is greatly improved (Figure 2c, Entry 10). Meanwhile, milder oxidant *p*-chloranil showed slightly improved performance compared with DDQ (Figure 2c, Entry 11). The purity of crude product could be up to 93 %, and it was much easier to wash out *p*-chloranil after the reaction, compared with the use of DDQ.

As the properties of porphyrins can be tuned by replacing the substituents on their *meso*-positions, we examined the substrate scope of various aldehydes and dipyrromethanes as the building blocks for constructing diverse porphyrin motifs on the model RGD peptide. Three simple aldehyde linkers were first investigated to couple with non-substituted dipyrromethane **1a**, giving the desired *trans*-divalent product **2b**–**2d** (Figure 3a and S4–S6). Either 2-(3-formylphenoxy)acetic acid (for constructing **2b**) or 3-formylbenzoic acid (for constructing **2d**) showed comparable conversion (> 85 %), which indicated that there was no apparent influence of the electron-withdrawing/donating groups (EWG/EDG) on the aldehyde linkers as mentioned

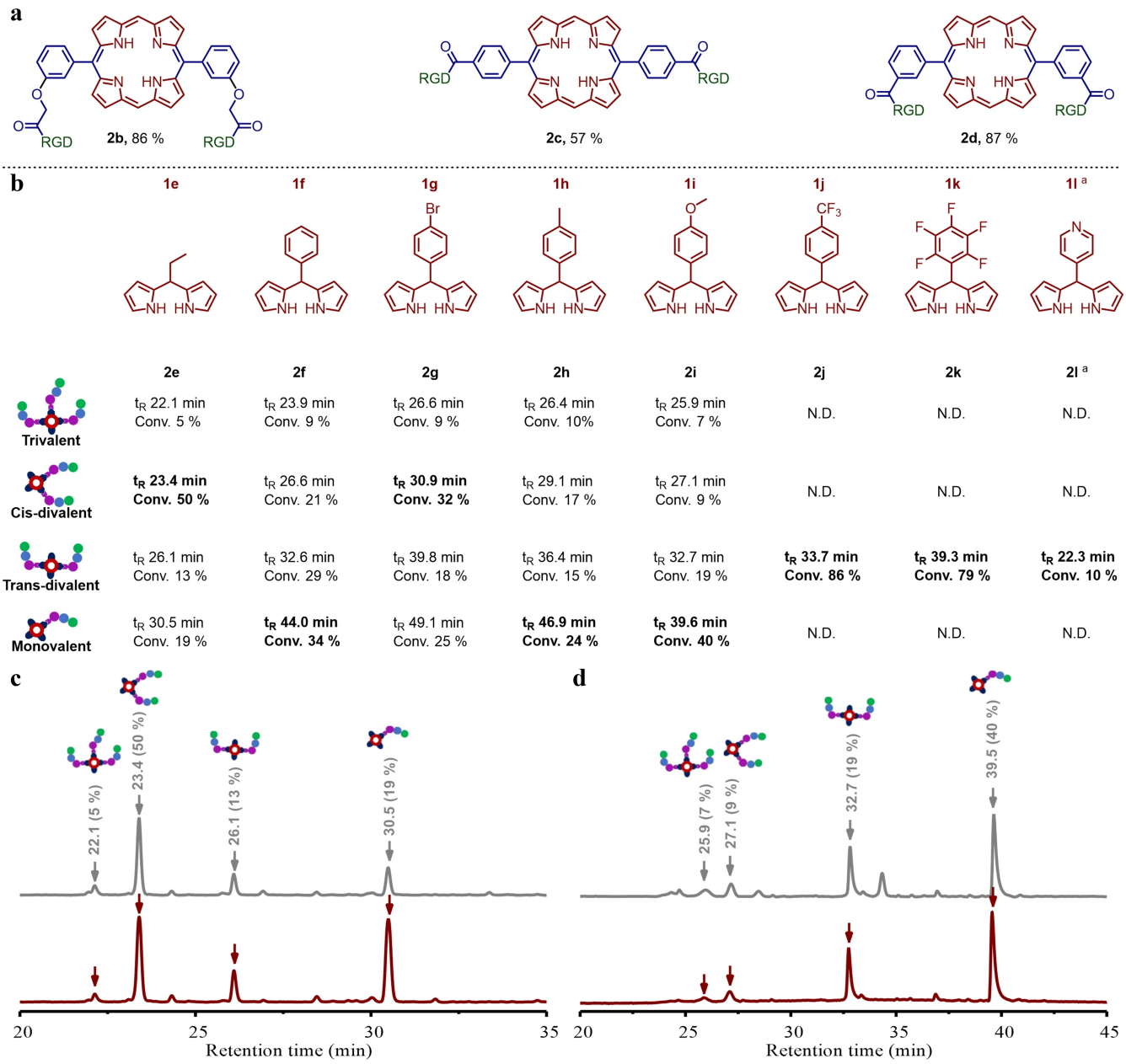

Figure 3. a) Construction of *trans*-divalent porphyrin–peptide conjugates by using different aldehyde linkers on the RGD peptide. b) Construction of porphyrins by using different dipyrromethanes on 2-(4-formylphenoxy)acetic acid coupled RGD peptide. The conversions were estimated by the HPLC (absorbance at 220 nm, which is mainly contributed by peptide bonds, thus, the conversions here reflect the percentage of peptide chain involved in corresponding product). [a] 5 equiv **1l** and 10 equiv; TFA was used (no conversion under 5 equiv TFA. c) The analytical HPLC of crude post-cleavage solution of **2e**. Absorbance at both 220 nm (grey) and 420 (maroon) are presented. The trivalent (t_R = 22.1 min), *cis*-divalent (t_R = 23.4 min), *trans*-divalent (t_R = 26.1 min) and monovalent (t_R = 30.5 min) porphyrin–peptide conjugates were isolated and identified. d) The analytical HPLC of crude post-cleavage solution of **2i**. Absorbance at both 220 nm (grey) and 420 (maroon) are presented. The trivalent (t_R = 25.9 min), *cis*-divalent (t_R = 27.1 min), *trans*-divalent (t_R = 32.7 min) and monovalent (t_R = 39.5 min) porphyrin–peptide conjugates were isolated and identified.

in the previous literature.[30] However, the efficiency of inter-peptide porphyrin construction decreased when 4-formylbenzoic acid (for constructing **2c**) was used. This might result from a lower probability for effective inter-peptide collision due to i) the relatively high rigidity, compared with 2-(3-formylphenoxy)acetic acid that would have two more rotatable bond, and ii) the unsuitable position, compared with 3-formylbenzoic acid that would allow two peptide chains to be coupled with smaller distortion, of its aldehyde linker.

A series of dipyrromethanes were then targeted for on-resin porphyrin construction (Figure 3b, S7–S14) to probe any substrate effects. Considerable conversions for *trans*-divalent porphyrin-peptide conjugates (>75 %, **2j** and **2k**)

could be achieved by using *meso*-EWG-substituted dipyrromethanes (**1j** and **1k**), while *meso*-pyridyl-substituted one (**1l**) led to a low conversion due to its intrinsic low reactivity (**2l**, 9 %).[31–33] Interestingly, using other *meso*-substituted dipyrromethanes containing more electron-donating substituents (**1e**–**1i**) resulted in complicated mixtures with multivalent porphyrin-peptide conjugates (**2e**–**2i**), which can be explained by the decomposition and recombination of these relatively unstable dipyrromethanes during the formation of porphyrin.[34] In these cases, other than the expected *trans*-divalent porphyrin-peptide conjugates, trivalent, *cis*-divalent, and monovalent ones (with 1–3 peptide chain on their porphyrin core) could all be isolated and identified. The *cis*-divalent porphyrin-peptide conjugates were formed as the primary products when the ethyl and 4-bromophenyl-substituted dipyrromethanes (**1e** and **1g**) were used, which showed relatively short retention time compared with the corresponding *trans*-divalent counterparts (Figure 3c). When the phenyl, 4-methylphenyl, and 4-methoxyphenyl-substituted dipyrromethanes were used (**1f**, **1h** and **1i**), the monovalent porphyrin-peptide conjugates, which have the longest retention time in crude mixture, can be constructed as the major product. In particular, for 4-methoxyphenyl-substituted dipyrromethanes (**1i)**, around 40 % of peptide chains were converted into the corresponding monovalent porphyrin conjugate. (Figure 3d). The trivalent porphyrin–peptide conjugates were found in all these cases as the minor products (Conv. $\leq$10 %). Additionally, trace amounts of dipyrrin-RGD conjugate can also be observed in these reactions (Conv. $\approx$5 %), which can be explained by the direct condensation between aldehyde and dissociated pyrrole.

These experiments displayed the potential of on-resin porphyrin construction as a practical protocol for labelling peptides with porphyrin motifs. On one hand, to synthesize *trans*-divalent porphyrin–peptide conjugates intentionally, the non-substituted/EWG-substituted dipyrromethanes can be applied. On the other hand, relatively unstable dipyrromethanes can be employed either to synthesize routinely used monovalent porphyrin–peptide conjugates or for fast establishment of libraries of porphyrin–peptide conjugates with different valency and configuration for studying the multivalent effect between the peptides and their corresponding targets.

As both monovalent and multivalent porphyrin–peptide conjugates are widely applied in previous literature studies, we therefore employed our protocol to synthesize a series of relatively long peptide chains with various well-known biomedical applications, including the nuclear localization sequence (NLS),[35,36] the mitochondrial localization sequence (MLS),[37–40] the STAT3-specific peptide, and the $\alpha_3\beta_v$-targeting cyclic peptide,[41–44] as well as their corresponding multi-/mono- valent peptide conjugates.

The non-substituted dipyrromethane (**1a**) was used at first to construct *trans*-divalent porphyrin–peptide conjugates (Figure 4a, S15, S19–S21). The conversions varied on different peptide sequences, and longer reaction time may be required in some cases. Although the length of peptide chains for synthesizing **3a**, **4**, and **5** are similar (7 amino acid residues for all three peptides), acceptable conversion can be achieved for **3a** (NLS peptide PKKKRKV, Conv. 81 %) and **4** (SATA3-specific peptide Ahx-PY*LKTK, Conv. 74 %) after 16 h condensation; however, less than 10 % of peptide chain was converted into **5** (the half sequence of MLS peptide KLAKLAK) under the identical condition. Longer reaction time was further tried for synthesizing **5**, and 65 % of conversion was achieved after 40 h condensation. The $\alpha_3\beta_v$-targeting cyclic(RGDyK) peptide on resin[45] was also used for inter-peptide porphyrin construction, and 21 % corresponding *trans*-divalent porphyrin–peptide conjugate (**6**) can be formed after 40 h condensation. For the cases with low conversion, pre-condensation peptides remained as main composition of their crude mixtures according to HPLC, and no significant porphyrin-containing by-products were observed. These results indicated the propensity of inter-peptide collision can be influenced by the length and amino acid composition (may lead to different secondary structures on resin) of the peptide chains.

The relatively unstable substituted dipyrromethanes was then used for constructing porphyrin motifs on/between these peptide chains (Figure 4b, S16–S18, S22, S23). For NLS peptide PKKKRKV, around 66 % of peptide chains was converted into corresponding monovalent conjugates (**3b**), while only 35 % of short RGD peptide can be converted into monovalent product (**2i**) by using the same aldehyde linker and dipyrromethane under the identical condition. The *trans*-divalent, *cis*-divalent and trivalent counterpart of **3b** were also observed with 12 % and 11 % conversions, respectively. Similarly, the ethyl-substituted dipyrromethane (**1e**) led to 25 % conversion of monovalent product (**3c**), which was also slightly higher than on RGD peptide (19 %). Interestingly, the conversion of monovalent product improved (**3d**, Conv. 35 %) when 4-formylbenzoic acid, which was regarded as a relatively unfavorable aldehyde linker for inter-peptide collision as mentioned previously, was used. The reactions were also conducted on the full sequence of MLS peptide $(KLAKLAK)_2$ with 14 amino acid residues, and acceptable conversions could be achieved for the corresponding monovalent products (21 % and 34 % for **7a** and **7b**, respectively), while the *trans*- and *cis*- divalent products were also identified with **7a** as the relatively minor products (Conv. 17 % and 7 %, respectively). The trivalent product was rarely observed in these cases, and the ratio of divalent products were also decreased compared with the similar reaction on short RGD peptide, indicating that the propensity of inter-peptide coupling decreased as the peptide chains elongated. The overall conversion of porphyrin–peptide conjugates also dropped as the formation of dipyrrin by-products boosted in the crude reacting mixture.

To examine the subcellular localization and the targeting effects of the synthesized porphyrin–peptide conjugates, a series of imaging experiments were conducted for **3a** (porphyrin-NLS conjugate), **5** & **7a** (porphyrin-MLS conjugates), as well as **6** ($\alpha_v\beta_3$-targetted porphyrin-cRGD conjugate).

The excitation and emission spectra of 10 μM **3a** (same chromophore in **5** and **6**) and **7a** in HEPES are showed in

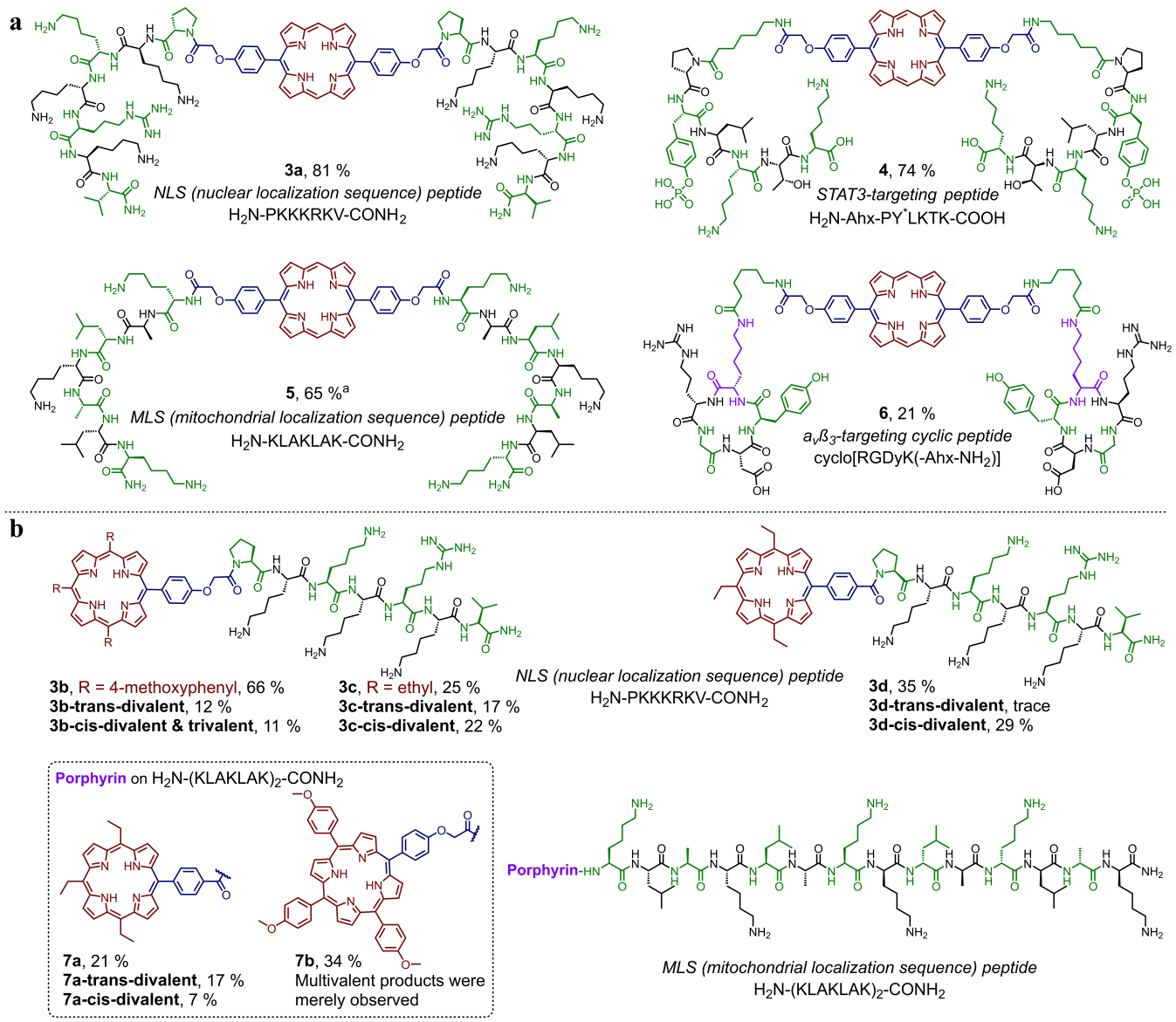

Figure 4. Construction of porphyrin–peptide conjugates on various bioactive peptides. The precent conversions are estimated by the HPLC according to the absorbance at 220 nm. a) The construction of *trans*-divalent porphyrin by using the non-substituted dipyrromethane (**1a**) on various peptide chains. b) The construction of monovalent porphyrin by using ethyl (**1e**) or 4-methoxyphenyl (**1i**) substituted dipyrromethane on various peptide chains.

Figure 5a and b, respectively. The typical red fluorescence (emission at 600–700 nm) of porphyrin derivatives can be observed under the excitation of a board range of wavelength. The divalent porphyrin-NLS conjugate **3a** was co-stained with NucBlueTM, a commonly used nucleus staining dye, in HeLa cell. As expected, both the red fluorescence from **3a** and the blue fluorescence from NucBlueTM were detected and well co-localized in the nucleus of HeLa cell line (Pearson's coefficient: 0.479) (Figure 5c). Similarly, the red fluorescence from the porphyrin motif of **5** and **7a** were found overlapped perfectly with the green color signals of the MitoTracker green in both HeLa and MDA-MD-231 cell lines (Pearson's coefficient: 0.403 and 0.341 respectively) (Figure 5d). These results exhibited the great potential for synthesized porphyrin–peptide conjugates as specific organelle dyes. Moreover, to demonstrate the specificity of synthesized compounds toward cancer biomarker, the immunoluminescence imaging of $\alpha_v\beta_3$-targetted porphyrin-cRGD conjugate **6** was also carried out in $\alpha_v\beta_3$ overexpressed breast cancer cell line MDA-MB-231 and $\alpha_v\beta_3$ non-overexpressed HeLa cell (Figure 5e). The fluorescent signals of **6** (red) showed significant overlapping with αvβ3-specific antibody (green) in MDA-MB-231 cell line (Pearson's coefficient: 0.405), while both signals were weakly observed in HeLa cell line. Such an adequate specificity enables the application of **6** as a promising $\alpha_v\beta_3$-targeting probe, thereby paving new ways for further developing **6** as a multifunc-

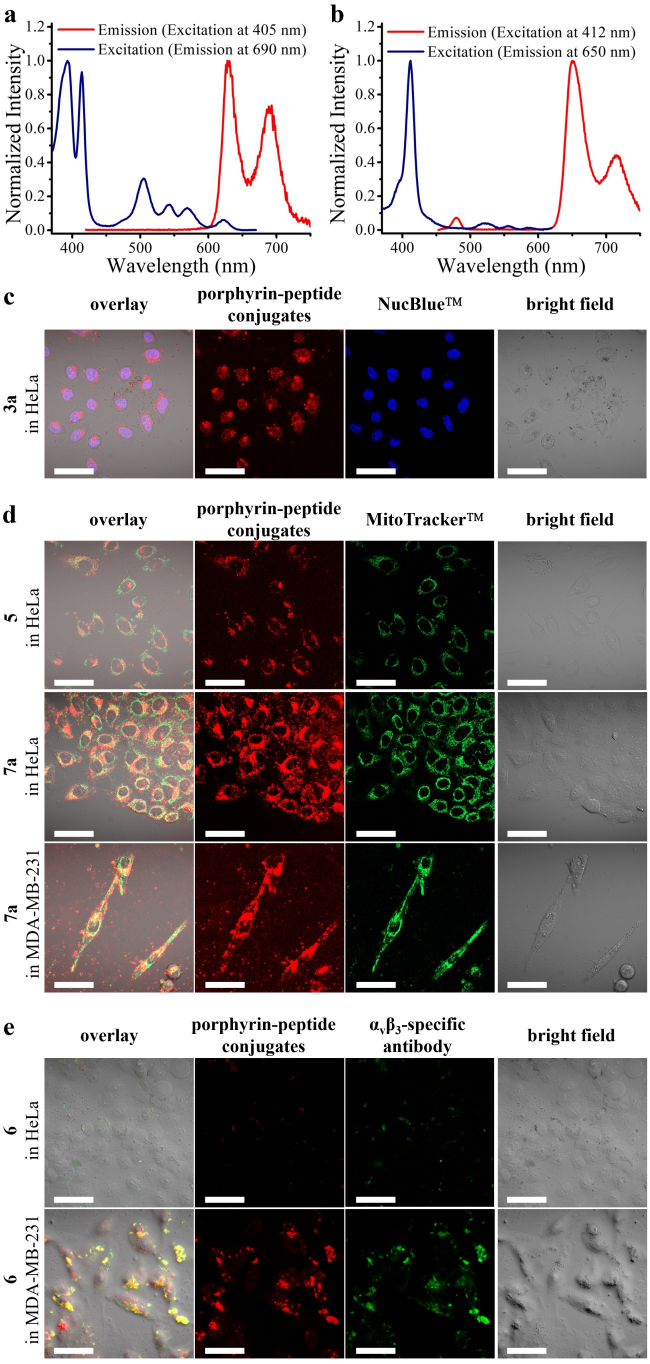

Figure 5. a) The normalized excitation and emission spectrum of 10 μM *trans*-divalent porphyrin–peptide conjugate **3a** in HEPES. b) The normalized excitation and emission spectrum of 10 μM monovalent porphyrin–peptide conjugate **7a** in HEPES. c) Confocal images of HeLa co-staining with NucBlue™ (nucleus staining dye with blue fluorescence) after incubation of 10 μM **3a** (porphyrin-NLS conjugate) for 24 h (scale bar: 25 mm). d) Confocal images of HeLa and MDA-MB-231 co-staining with MitoTracker™ (mitochondria dye with green fluorescence) after incubation of 5 μM **5** and **7a** (porphyrin-MLS conjugates) for 24 h (scale bar: 25 mm). e) Immunoluminescence imaging of $\alpha_v\beta_3$ in HeLa ($\alpha_v\beta_3-$) and MDA-MD-231 ($\alpha_v\beta_3+$) after incubation of 5 μM **6** (porphyrin-cRGD conjugate) for 24 h (scale bar: 25 mm).

tional $\alpha_v\beta_3$-selective fluorescence imaging and photodynamic therapy theranostic dual-agent.

Conclusion

A novel, efficient and practical solid-phase controllable synthetic methodology has been developed to yield bioactive multivalent porphyrin–peptide conjugates without using pre-functionalized porphyrin building blocks and tedious multi-step purifications. By coupling two peptide chains on resin with stable electron-deficient dipyrromethanes, the *trans*-divalent porphyrin–peptide conjugates can be obtained with considerable yields. Moreover, by making use of the decomposition and recombination of relatively unstable electron-rich dipyrromethanes, the porphyrin–peptide conjugates with different valency and configurations can be obtained in a single reaction, which enables either the fast investigation of the multivalent effect of the peptides toward their corresponding targets or facile preparation of most frequently used monovalent porphyrin–peptide conjugates. A series of porphyrin-(long) peptide conjugates, exhibiting expected photophysical and biomedical applications, have been obtained by using this protocol for the model studies. Our protocol can strategically provide a new synthetic platform (which can be promisingly incorporated into future automated continuous flow synthesis) to expeditiously establish diversity-oriented synthesis libraries of porphyrin-(long) peptide conjugates, thereby supporting theranostics/drug discovery and development, as well as advanced materials research.

Acknowledgements

Financial assistances from the Hong Kong Research Grants Council No. 12300021, Dr Mok Man Hung Endowed Professorship in Chemistry, HKBU-Durham Lanthanide Joint Research Center—Lanthanide Tools for Systems Medicine (SDF19-1011-P02) and the Centre for Medical Engineering of Molecular and Biological Probes (AoE/M-401/20) are gratefully acknowledged (K.-L.W). W.-L.C. was financially supported by the Hong Kong Polytechnic University (Start-up Fund for RAPs under the Strategic Hiring Scheme P0035714). We appreciate Ho-Nam Mak and Kwok-Ho Lui from the Department of Applied Biology and Chemical Technology of The Hong Kong Polytechnic University for the trials of nanoparticle formation for our synthesized compounds.

Conflict of Interest

The authors declare no conflict of interest.

Data Availability Statement

The data that support the findings of this study are available in the Supporting Information of this article.

Keywords: Fluorescent Peptides · Multivalent Porphyrin–Peptide Conjugates · Porphyrins · Solid-Phase Peptide Synthesis · Targeted Bioimaging

[1] J. F. Arambula, J. L. Sessler, *Chem* **2020**, *6*, 1634–1651.
[2] F. Biscaglia, M. Gobbo, *Pept. Sci.* **2018**, *110*, e24038.
[3] P. Pathak, M. A. Zarandi, X. Zhou, J. Jayawickramarajah, *Front. Chem.* **2021**, *9*, 764137.
[4] P. Agostinis, K. Berg, K. A. Cengel, T. H. Foster, A. W. Girotti, S. O. Gollnick, S. M. Hahn, M. R. Hamblin, A. Juzeniene, D. Kessel, M. Korbelik, J. Moan, P. Mroz, D. Nowis, J. Piette, B. C. Wilson, J. Golab, *Ca-Cancer J. Clin.* **2011**, *61*, 250–281.
[5] D. E. J. G. J. Dolmans, D. Fukumura, R. K. Jain, *Nat. Rev. Cancer* **2003**, *3*, 380–387.
[6] Á. Juarranz, P. Jaén, F. Sanz-Rodríguez, J. Cuevas, S. González, *Clin. Transl. Oncol.* **2008**, *10*, 148–154.
[7] F. Nastri, M. Chino, O. Maglio, A. Bhagi-Damodaran, Y. Lu, A. Lombardi, *Chem. Soc. Rev.* **2016**, *45*, 5020–5054.
[8] C. J. Reedy, B. R. Gibney, *Chem. Rev.* **2004**, *104*, 617–649.
[9] R. Zou, J. Huang, J. Shi, L. Huang, X. Zhang, K. L. Wong, H. Zhang, D. Jin, J. Wang, Q. Su, *Nano Res.* **2017**, *10*, 2070–2082.
[10] X. Xue, A. Lindstrom, Y. Li, *Bioconjugate Chem.* **2019**, *30*, 1585–1603.
[11] B. Sun, K. Tao, Y. Jia, X. Yan, Q. Zou, E. Gazit, J. Li, *Chem. Soc. Rev.* **2019**, *48*, 4387–4400.
[12] P. Dognini, C. R. Coxon, W. A. Alves, F. Giuntini, *Molecules* **2021**, *26*, 693.
[13] G. Charalambidis, E. Georgilis, M. K. Panda, C. E. Anson, A. K. Powell, S. Doyle, D. Moss, T. Jochum, P. N. Horton, S. J. Coles, M. Linares, D. Beljonne, J. V. Naubron, J. Conradt, H. Kalt, A. Mitraki, A. G. Coutsolelos, T. S. Balaban, *Nat. Commun.* **2016**, *7*, 12657.
[14] B. Sun, R. Chang, S. Cao, C. Yuan, L. Zhao, H. Yang, J. Li, X. Yan, J. C. M. van Hest, *Angew. Chem. Int. Ed.* **2020**, *59*, 20582–20588; *Angew. Chem.* **2020**, *132*, 20763–20769.
[15] P. Ruzza, A. Marchiani, N. Antolini, A. Calderan, *Anti-Cancer Agents Med. Chem.* **2012**, *12*, 416–427.
[16] M. Lelle, C. Freidel, S. Kaloyanova, K. Müllen, K. Peneva, *Int. J. Pept. Res. Ther.* **2018**, *24*, 355–367.
[17] B. Cen, Y. Wei, W. Huang, M. Teng, S. He, J. Li, W. Wang, G. He, X. Bai, X. Liu, Y. Yuan, X. Pan, A. Ji, *Mol. Ther. Nucleic Acids* **2018**, *13*, 220–232.
[18] A. N. Singh, M. J. McGuire, S. Li, G. Hao, A. Kumar, X. Sun, K. C. Brown, *Theranostics* **2014**, *4*, 745–760.
[19] X. Xie, J. He, *Eur. J. Med. Chem.* **2022**, *230*, 114140.
[20] A. Borbély, F. Thoreau, E. Figueras, M. Kadri, J. L. Coll, D. Boturyn, N. Sewald, *Chem. Eur. J.* **2020**, *26*, 2602–2605.
[21] I. Dijkgraaf, A. Y. Rijnders, A. Soede, A. C. Dechesne, G. W. Van Esse, A. J. Brouwer, F. H. M. Corstens, O. C. Boerman, D. T. S. Rijkers, R. M. J. Liskamp, *Org. Biomol. Chem.* **2007**, *5*, 935–944.
[22] L. Li, B. P. Orner, T. Huang, A. P. Hinck, L. L. Kiessling, *Mol. BioSyst.* **2010**, *6*, 2392–2402.
[23] F. Giuntini, C. M. A. Alonso, R. W. Boyle, *Photochem. Photobiol. Sci.* **2011**, *10*, 759–791.
[24] R. B. Merrifield, *J. Am. Chem. Soc.* **1963**, *85*, 2149–2154.
[25] M. Amblard, J. A. Fehrentz, J. Martinez, G. Subra, *Mol. Biotechnol.* **2006**, *33*, 239–254.
[26] J. M. Palomo, *RSC Adv.* **2014**, *4*, 32658–32672.
[27] Y. Wu, W. S. Tam, H. F. Chau, S. Kaur, W. Thor, W. S. Aik, W. L. Chan, M. Zweckstetter, K. L. Wong, *Chem. Sci.* **2020**, *11*, 11266–11273.
[28] Y. Wu, H. F. Chau, W. Thor, K. H. Y. Chan, X. Ma, W. L. Chan, N. J. Long, K. L. Wong, *Angew. Chem. Int. Ed.* **2021**, *60*, 20301–20307; *Angew. Chem.* **2021**, *133*, 20463–20469.
[29] J. S. Manka, D. S. Lawrence, *Tetrahedron Lett.* **1989**, *30*, 6989–6992.
[30] Z. Abada, L. Ferrié, B. Akagah, A. T. Lormier, B. Figadre, *Tetrahedron Lett.* **2011**, *52*, 3175–3178.
[31] M. Boccalon, E. Iengo, P. Tecilla, *J. Am. Chem. Soc.* **2012**, *134*, 20310–20313.
[32] H. Wu, F. Yang, X. L. Lv, B. Wang, Y. Z. Zhang, M. J. Zhao, J. R. Li, *J. Mater. Chem. A* **2017**, *5*, 14525–14529.
[33] H. Nobukuni, Y. Shimazaki, F. Tani, Y. Naruta, *Angew. Chem. Int. Ed.* **2007**, *46*, 8975–8978; *Angew. Chem.* **2007**, *119*, 9133–9136.
[34] G. R. Geier, J. S. Lindsey, *Tetrahedron* **2004**, *60*, 11435–11444.
[35] M. Sibrian-Vazquez, T. J. Jensen, M. G. H. Vicente, *Org. Biomol. Chem.* **2010**, *8*, 1160–1172.
[36] I. Sehgal, M. Sibrian-Vazquez, M. G. H. Vicente, *J. Med. Chem.* **2008**, *51*, 6014–6020.
[37] M. Sibrian-Vazquez, I. V. Nesterova, T. J. Jensen, M. G. H. Vicente, *Bioconjugate Chem.* **2008**, *19*, 705–713.
[38] G. A. Johnson, N. Muthukrishnan, J. P. Pellois, *Bioconjugate Chem.* **2013**, *24*, 114–123.
[39] H. Tong, J. Du, H. Li, Q. Jin, Y. Wang, J. Ji, *Chem. Commun.* **2016**, *52*, 11935–11938.
[40] K. Han, Q. Lei, S. B. Wang, J. J. Hu, W. X. Qiu, J. Y. Zhu, W. N. Yin, X. Luo, X. Z. Zhang, *Adv. Funct. Mater.* **2015**, *25*, 2961–2971.
[41] V. Chaleix, V. Sol, Y. M. Huang, M. Guilloton, R. Granet, J. C. Blais, P. Krausz, *Eur. J. Org. Chem.* **2003**, 1486–1493.
[42] M. Sibrian-Vazquez, X. Hu, T. J. Jensen, M. G. H. Vicente, *J. Porphyrins Phthalocyanines* **2012**, *16*, 603–615.
[43] C. L. Conway, I. Walker, A. Bell, D. J. H. Roberts, S. B. Brown, D. I. Vernon, *Photochem. Photobiol. Sci.* **2008**, *7*, 290–298.
[44] C. Frochot, B. Di Stasio, R. Vanderesse, M. J. Belgy, M. Dodeller, F. Guillemin, M. L. Viriot, M. Barberi-Heyob, *Bioorg. Chem.* **2007**, *35*, 205–220.
[45] A. Del Gatto, M. De Simone, I. De Paola, M. Saviano, L. Zaccaro, *Int. J. Pept. Res. Ther.* **2011**, *17*, 39–45.

Manuscript received: May 23, 2022
Accepted manuscript online: June 22, 2022
Version of record online: July 11, 2022